Structures of stable oxide cluster ions of first-row late transition metals: An ion mobility-mass spectrometric study

Structures of stable oxide cluster ions of first-row late transition metals: An ion mobility-mass spectrometric study

Fuminori Misaizu, M. Abdul Latif, Jenna W. J. Wu, Ryoichi Moriyama, Motoyoshi Nakano, Kiichirou Koyasu, and Keijiro Ohshimo

View Online   Export Citation

ARTICLES YOU MAY BE INTERESTED IN

Structures of Stable Oxide Cluster Ions of First-Row Late Transition Metals: An Ion Mobility-Mass Spectrometric Study

Fuminori Misaizu[1, a)], M. Abdul Latif[1, 2], Jenna W. J. Wu[1], Ryoichi Moriyama[1], Motoyoshi Nakano[1], Kiichirou Koyasu[1], and Keijiro Ohshimo[1]

[1] *Department of Chemistry, Graduate School of Science, Tohoku University, Sendai 980-8578, Japan*
[2] *Department of Chemistry, Faculty of Science, Begum Rokeya University, Rangpur-5400, Bangladesh*

a) Corresponding author: misaizu@m.tohoku.ac.jp

Abstract. Ion mobility mass spectrometry has been applied to unveil stable compositions and geometrical structures of oxide cluster ions of first-row late transition metals such as Fe, Co, Ni, Cu, and Zn. Geometrical structures were assigned by comparison of collision cross sections obtained by this experiment with those calculated for the structures predicted by quantum chemical calculations. Mass spectra of stable compositions of the metal oxide cluster ions resulting from collision-induced-dissociation in the ion drift cell have also been obtained. Oxides of the late transition metals except for Cu were found to have common stable compositions with the same numbers of metal and oxygen atoms, $(FeO)_n^+$, $(CoO)_n^+$, $(NiO)_n^+$, and $(ZnO)_n^+$, in addition to oxygen-rich $Fe_nO_{n+1}^+$ ions or oxygen-deficient $Co_nO_{n-1}^+$, $Ni_nO_{n-1}^+$, and $Zn_nO_{n-1}^+$ ions for n up to ≈ 10. As for the copper oxide clusters, $Cu_nO_m^+$ ions with $n{:}m \approx 2{:}1$ were predominant in the mass spectrum. For the stable ions, structural transitions were commonly observed from two-dimensional (2D) cyclic or sheet structures to three-dimensional (3D) compact structures at around the size n smaller than 8. Both types of isomers coexist at $n = 6\text{-}8$ for $(FeO)_n^+$ and $(ZnO)_n^+$, and at $n = 5$ for $(NiO)_n^+$, whereas 3D structures were clearly observed from $n = 6$ for $(CoO)_n^+$. These structural transitions were characteristic for the oxide cluster ions of the late transition metals, in marked contrast to those of early transition metals.

INTRODUCTION

Metal oxide nanoparticles are regarded not only as local structure models of solids or surfaces but also as candidates of novel functional materials. In particular, nanoparticles of transition metal oxides are now widely utilized as catalysts, materials of electronic devices, magnetic storage media, and so on. The possibility of application of smaller sized particles, that is, nanoclusters or clusters, is also pursued extensively in the past few decades. It is important to investigate the size-dependent change of properties of the clusters, since most of the properties have strong size dependence. In addition, there are some structural isomers even if the cluster size was selected. Therefore, it is necessary to investigate the size- and isomer-selected clusters to unveil the pure properties of the clusters.

Spectroscopic techniques such as infrared spectroscopy and photoelectron spectroscopy have been applied for the determination of cluster structures. However, it is a long way to obtain the spectra of wide range of size-selected clusters. On the other hand, ion mobility spectrometry, which is an analytical and separation method using interaction of the target ions with buffer gas, is also a powerful method to assign geometrical structures of cluster ions in the wide size range from the determination of collision cross sections (CCSs). For the purpose of identifying cluster ion structures, ion mobility mass spectrometry (IM-MS), which is a combination of ion mobility spectrometry and mass spectrometry, was applied to various cluster ions such as metal clusters [1], group 14 clusters [2], ionic nanocrystals [3], molecular clusters [4], and also metal oxide clusters [5].

We have applied IM-MS to investigate stable compositions and geometrical structures of oxide cluster ions of first-row late transition metals, Fe [6], Co [7], Ni [8], Cu [9] and Zn [10]. In the present paper, we showed the results of the structure assignments for oxygen-equivalent cluster ions, $(FeO)_n^+$, $(CoO)_n^+$, $(NiO)_n^+$, and $(ZnO)_n^+$. This is the first comparative study of the structures of these metal oxide cluster ions, whereas such comparison was reported theoretically for neutral clusters [11].

EXPERIMENTAL AND THEORETICAL METHODS

Experiment was performed in a vacuum apparatus containing a cluster ion source, an ion-drift cell for ion mobility spectrometry, and a reflectron-type time-of-flight mass spectrometer (TOF-MS). The setup was already reported in detail elsewhere [5-10]. Metal oxide cluster cations were produced by laser vaporization of a metal rod and subsequent reaction with O_2 gas seeded in He which was expanded from a pulsed valve. The generated cluster ions were injected into the ion-drift cell with a given kinetic energy E_{inj} between 50-250 eV by a pulsed electric field. The ion-drift cell was filled with He buffer gas at 0.80 or 0.90 Torr and was cooled to 190 K. The ions were accelerated by the electrostatic field ($E = 10$ V/cm) in the drift cell. As a result of the balance between the collisions and electrostatic acceleration, the ions reached a constant drift velocity v_d which is proportional to E, that is, $v_d = KE$. Here the coefficient K is called ion mobility. After exiting the cell, the ions were re-accelerated in an acceleration region of the reflectron TOF-MS at a given time Δt later from the ion-injection pulse. This delay time, Δt, was hereafter denoted as "arrival time". Finally, the ions were mass-analyzed by the TOF-MS. In the IM-MS measurement, we obtained a series of TOF mass spectra sequentially by scanning Δt. As a result, cluster ions with different cross sections were separately detected at different arrival times in a two-dimensional (2D) plot of TOF vs. arrival time.

The collision cross section Ω between the ion and a He atom was determined from the measurement of the ion mobility K using the following Eq. (1) based on the theory of ion transport [12].

$$K = \frac{3e}{16N} \left(\frac{2\pi}{k_B \mu T_{eff}} \right)^{1/2} \frac{1}{\Omega}, \tag{1}$$

where e is the elementary charge, N is the number density of the buffer gas, k_B is the Boltzmann constant, μ is the reduced mass of the ion and the buffer gas atom. The term T_{eff}, the effective temperature of the ions, is given by $T_{BG} + m_B v_d^2/3k_B$, where T_{BG} is the buffer gas temperature and m_B is the mass of buffer gas. The ion flight time in the drift cell t_d was first determined by subtracting the time flying the outside regions of the cell, which was calculated with solving the equations of motion of the ions, from the peak of the arrival time distribution of the ion. Then the drift velocity v_d and thus the ion mobility K were determined from t_d. Finally, Ω was determined from the Eq. (1). A TOF mass spectrum was also obtained from the 2D plot of TOF vs. arrival time noted above. In the present apparatus, after injection into the cell by a pulsed electric field, cluster ions diffuse spatially in their running direction depending on their cross sections before reaching the acceleration region of the TOF mass spectrometer. Therefore, the TOF mass spectrum was obtained by summing up all the TOF spectra measured at every arrival time because of the spread of arrival time distribution of the cluster ions.

Quantum chemical calculations for the geometry optimizations of metal oxide cluster ions were performed prior to calculations of collision integrals which can be compared with the CCSs of the ions. The geometry optimizations were carried out with 6-311+G(d) (Zn oxides) or 6-31+G(d) (Fe, Co, and Ni oxides) basis sets and B3LYP functional in Gaussian 09. Several spin states were examined in these calculations. The CCS of the ion with a He atom was calculated by the projection approximation method which is included in the MOBCAL program [13].

RESULTS AND DISCUSSION

Stable Compositions of Metal Oxide Cluster Ions

The observed cluster-ion compositions were strongly dependent on the ion injection energy E_{inj} to the ion-drift cell. In general, a few series of cluster ions were observed in the TOF mass spectra at high ion injection energy ($E_{inj} = 250$ eV) as shown in **FIGURE 1**. This is a result of collision induced dissociation just after injection into the ion-drift cell as discussed in previous papers [14], and therefore, the ions survived at high injection energies are stable compositions with respect to dissociation.

As a result, oxygen-equivalent cluster ions such as $(FeO)_n^+$, $(CoO)_n^+$, and $(NiO)_n^+$ were observed in these mass spectra. This result reflects that the late transition metals in general have an oxidation number of +2, although one electron is lacking in these singly charged cluster ions. In addition, one oxygen-rich series, $Fe_nO_{n+1}^+$, was also

observed for iron oxide cluster ions, due to the contribution of iron oxidation number of +3. By contrast, one oxygen-poor series, $Co_nO_{n-1}^+$ and $Ni_nO_{n-1}^+$, were also predominantly observed for Co and Ni oxide cluster ions, probably because of the total positive charge of the ions. As for the anions of these metal oxide clusters, more oxygen-rich clusters were observed as stable compositions. Also for the zinc oxide cluster ions, the $(ZnO)_n^+$ ions were exclusively observed in the mass spectrum under the similar conditions of **FIGURE 1** [10], which reflects the fact that the zinc has only an oxidation number of +2 in bulk compounds. Copper oxide cluster ions have, on the other hand, main compositions of $Cu_nO_{n/2}^+$ and neighboring series, which are probably due to the oxidation number of +1 of the copper atom [9].
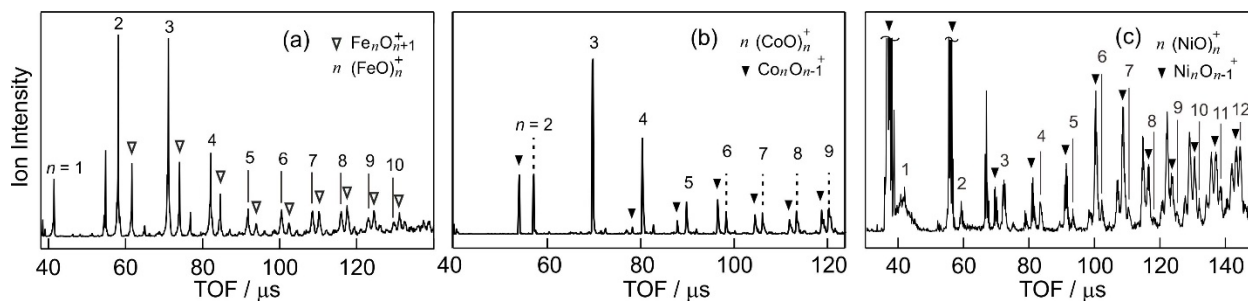

FIGURE 1. TOF mass spectra of cluster ions of (a) iron oxide, (b) cobalt oxide, and (c) nickel oxide with an ion-injection energy of 250 eV to the ion-drift cell. The pressures of the drift cell were 0.80 Torr for (a) and (b), and 0.90 Torr for (c). The cell temperature was kept at 190 K.

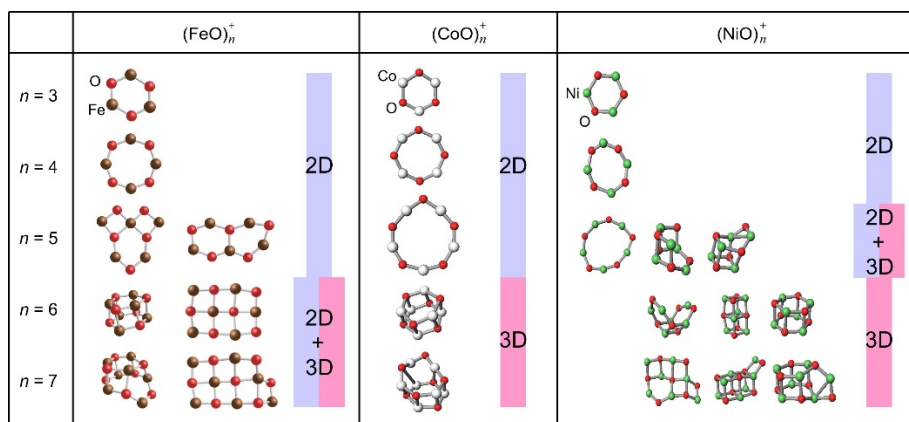## Collision Cross Sections (CCSs) and Structures of Metal Oxide Cluster Ions

FIGURE 2. Typical structures of $(FeO)_n^+$, $(CoO)_n^+$, and $(NiO)_n^+$ cluster ions for $n = 3$-7. These structures were assigned from the comparison between the CCSs determined by IM-MS measurements and those of the optimized structures by DFT calculations. 2D to 3D structural change was commonly found at $n = 5$ or 6 with increasing cluster size.

Here we summarized qualitatively the changes of the assigned structures of oxygen-equivalent metal oxide cluster ions, $(FeO)_n^+$, $(CoO)_n^+$, $(NiO)_n^+$, and $(ZnO)_n^+$, which are the stable compositions as noted above, with increasing cluster size up to $n = 8$. Typical structures for the former three cluster ions for $n = 3$-7 are shown in **FIGURE 2**, which were assigned from the comparison between the CCSs determined by IM-MS measurements and those of the optimized structures by DFT calculations. These structures were obtained for the cluster ions with different spin states, although the relative energy was dependent on the spin states. As for $(FeO)_n^+$, the ions were assigned to have 2D ring structures for $n = 3$-5, whereas three-dimensional (3D) tower structures exist in addition to 2D sheet isomers for $n = 6$ and 7. Similar isomer coexistence was also found for $(FeO)_8^+$. On the other hand, 2D to 3D structure change was clearly observed between $n = 5$ and 6 for $(CoO)_n^+$. Similar structural change was also

observed for $(NiO)_n^+$, excepting the 2D and 3D isomer coexistence at $n = 5$. Also for $(ZnO)_n^+$, similar change was discerned, and both 2D and 3D structures were found at $n = 6\text{-}8$. Therefore, structure transitions from 2D to 3D were commonly found at $n = 5$ or 6 with increasing cluster size for these oxygen-equivalent cluster ions of the late transition metal oxides. Another common feature in the structures of these metal oxide cluster ions is that the oxygen atoms are bridged between two metal atoms. This feature is a result of ionic bond nature between doubly charged metal atomic ions and O^{2-}. In fact, these structural features showed marked contrast with the oxide cluster ions of early transition metals, such as $(TiO_2)_n^+$ [5], $(V_2O_5)_{n/2}^+$ [15], and $(CrO_2)_n^+$ [16], and also with $Cu_nO_{n/2}^+$ ions [9]. The latter ions have more oxygen atoms than the metal atoms, and the oxygen atoms in most of the cluster ions are again bridged between metal atoms. Therefore, 3D complicated structures were already formed even at the smallest cluster size in the ions of these early transition metal oxides.

ACKNOWLEDGMENTS

REFERENCES

1. S. Gilb, P. Weis, F. Furche, R. Ahlrichs, and M. M. Kappes, J. Chem. Phys. **116**, 4094–4101 (2002).
2. G. von Helden, P. R. Kemper, N. G. Gotts, and M. T. Bowers, Science **259**, 1300–1302 (1993).
3. R. R. Hudgins, P. Dugourd, J. M. Tenenbaum, and M. F. Jarrold, Phys. Rev. Lett. **78**, 4213–4216 (1997).
4. M. J. Rusyniak, Y. M. Ibrahim, D. L. Wright, S. N. Khanna, and M. S. El-Shall, J. Am. Chem. Soc. **125**, 12001–12013 (2003).
5. K. Ohshimo, N. Norimasa, R. Moriyama, and F. Misaizu, J. Chem. Phys. **144**, 194305 (2016). (8 pages)
6. K. Ohshimo, T. Komukai, R. Moriyama, and F. Misaizu, J. Phys. Chem. A **118**, 3899–3905 (2014).
7. K. Ota, K. Koyasu, K. Ohshimo, and F. Misaizu, Chem. Phys. Lett. **588**, 63–67 (2013).
8. K. Ohshimo, S. Azuma, T. Komukai, R. Moriyama, and F. Misaizu, J. Phys. Chem. C **119**, 11014–11021 (2015).
9. M. A. Latif, J. W. J. Wu, R. Moriyama, M. Nakano, K. Ohshimo, and F. Misaizu, ACS Omega **3**, 18705–18713 (2018).
10. K. Koyasu, K. Komatsu, and F. Misaizu, J. Chem. Phys. **139**, 164308 (2013). (6 pages)
11. G. L. Gutsev, K. G. Belay, K. V. Bozhenko, L. G. Gutsev, and B. R. Ramachandran, Phys. Chem. Chem. Phys. **18**, 27858-27867 (2016).
12. E. A. Mason and E. W. McDaniel, *Transport Properties of Ions in Gases* (Wiley and Sons, New York, 1988).
13. M. F. Mesleh, J. M. Hunter, A. A. Shvartsburg, G. C. Schatz, and M. F. Jarrold, J. Phys. Chem. **100**, 16082–16086 (1996).
14. K. Ohshimo, T. Takahashi, R. Moriyama, and F. Misaizu, J. Phys. Chem. A **118**, 9970–9975 (2014).
15. J. W. J. Wu, R. Moriyama, H. Tahara, K. Ohshimo, and F. Misaizu, J. Phys. Chem. A **120**, 3788–3796 (2016).
16. R. Moriyama, R. Sato, M. Nakano, K. Ohshimo, and F. Misaizu, J. Phys. Chem. A **121**, 5605–5613 (2017).